Dynamic Telemetry Bit Rates for Deep Space Communications

Jeff B. Berner	Mail Stop 238-737 Jet Propulsion Laboratory 4800 Oak Grove Drive Pasadena, CA 91109-8099	(818) 354-3934 phone (818) 354-2825 fax jeff.berner@jpl.nasa.gov
Peter W. Kinman	Electrical Engineering Case Western Reserve University Cleveland, OH 44106-7221	(216) 368-5550 phone (216) 368-2668 fax pwk@eecs.cwru.edu
Miles K. Sue	Mail Stop 161-260 Jet Propulsion Laboratory 4800 Oak Grove Drive Pasadena, CA 91109-8099	(818) 354-4394 phone (818) 393-4643 fax miles.sue@jpl.nasa.gov

Designated Presenter: Jeff B. Berner
Technical Subject Area: Satellite and Space Communications

Abstract

A new telemetry playback scheme promises to maximize telemetry return for deep space missions. For a given effective isotropic radiated power from the spacecraft, the received signal-to-noise spectral density ratio and hence the supportable bit rate vary during a tracking pass as the elevation angle changes. In the past, spacecraft would use just one bit rate or perhaps a few different bit rates during a pass. However, large bit rate changes sometimes cause the ground receiver to go out of lock. The new scheme, which is examined here, allows the spacecraft to change its bit rate in frequent, small steps to match the signal-to-noise spectral density ratio profile. Because the rate changes are small, the ground receiver will be able to remain in lock.

Jeff Berner will attend ICC in New Orleans if this paper is accepted.

1 Introduction

The profile with which the received downlink total power to noise spectral density ratio (P_T/N_0) varies during a tracking pass is largely predictable, resulting as it does from the well-defined progression from low elevation angle to high and back to low. Figure 1 shows an example P_T/N_0 profile for an X-band downlink. This curve represents a typical profile when tracking a spacecraft with 25° declination.[1] If the telemetry bit rate is dynamically changed to follow the P_T/N_0 profile, so that a relatively large bit rate is used near zenith and relatively small bit rates are used near the beginning and end of the pass when the elevation angle is low, then it is possible to maximize the number of total bits returned during the tracking pass.

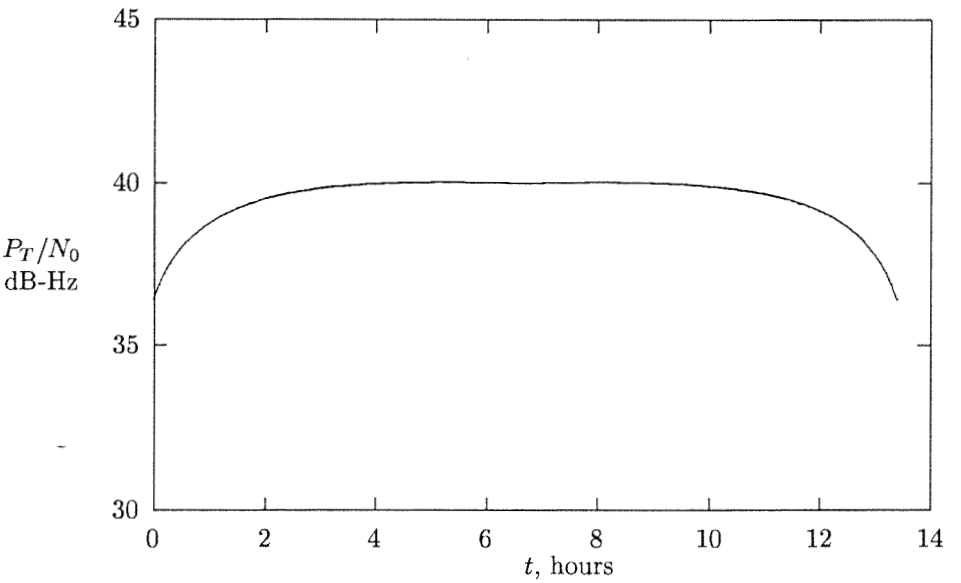

Figure 1: Example X-band P_T/N_0 curve

A typical telemetry signal structure for deep space communications is considered here. The information bits are encoded using a convolutional code, the binary symbols out of the encoder are phase-reversal keyed onto a squarewave subcarrier, and the modulated subcarrier is phase modulated onto a carrier with a modulation index of less than 90°, so that a residual carrier is present. The residual carrier is used by the receiver for carrier synchronization. The subcarrier frequency is harmonically related to the symbol rate, so both the subcarrier frequency and symbol rate change together. The telemetry link is line-of-sight between spacecraft and Deep Space Network antenna, and the performance is limited by thermal noise, which is well modeled as additive, white and Gaussian.

The challenge for the receiver is to maintain subcarrier lock and symbol lock despite changes in the subcarrier frequency and symbol rate. If either of these loops loses lock, then succeeding stages — the node synchronizer in the Viterbi decoder and the frame synchronizer — will be impacted. If enough time is lost in the reacquisition, there is no net advantage to be gained by changing the bit rate.

In principle, if sufficiently accurate predictions of the subcarrier frequency and symbol-rate changes are made available to the receiver, the subcarrier and symbol loops can be programmed to follow the changes with minimal probability of falling out of lock, even if the changes are large. Often, however, it will be impractical to deliver predictions of subcarrier frequency and symbol rate change that are of sufficient accuracy to the receiver. This will especially be true in the case of higher bit rates.

In the remainder of this paper it is assumed that only relatively coarse subcarrier frequency and symbol rate predictions are made available to the receiver. These coarse predictions are needed for acquisition. But the predictions are assumed to be inadequate for a programmed tracking of the subcarrier frequency and symbol rate. It is assumed that the clock onboard the spacecraft that determines subcarrier frequency and symbol rate has a continuous phase; the rate-of-change of its phase will abruptly change, but its phase will be always continuous.

The telemetry playback scheme to be examined in this paper is now explained. The bit rate is changed in small steps; these steps occur periodically. Each step in bit rate is effected by a (phase-continuous) step in the frequency of the spacecraft clock that determines symbol rate and subcarrier frequency. The steps are small enough that neither the subcarrier loop nor the symbol loop loses lock. The receiver can therefore track the downlink without having access to precise predictions of these phase-rate changes.

This scheme is attractive because it does not require the kind of precise predictions that are required if the bit rate is changed in big steps. However, there is also a disadvantage to this scheme. If during a tracking pass the subcarrier or the symbol loop should lose lock and reacquisition should become necessary, then there are some complications. But that should be a rare event.

In the section immediately following, the achievable static bit rate is related to P_T/N_0 for the case of residual-carrier telemetry. In the section after that, the transient responses of subcarrier and symbol loops to an isolated phase-rate step and also to a periodic series of phase-rate steps are calculated. These calculations provide guidance to the size and the frequency of bit rate steps that are possible. With this preliminary material as background, it then becomes possible to calculate the total data return for the proposed telemetry playback scheme with dynamic bit rate. Similar results for the case of suppressed-carrier telemetry have been reported elsewhere.[2]

2 Achievable Bit Rate for Residual-Carrier Telemetry

For a given P_T/N_0, the largest bit rate that may be supported depends on the code being used, the threshold bit error rate (BER), as well as several receiver parameters. The following paragraphs characterize these relationships. Only two codes are considered in this paper: the CCSDS (Consulatative Committee on Space Data Systems) standard constraint length 7, rate 1/2, convolutional code (7, 1/2) and a constraint length 15, rate 1/6, convolutional code (15, 1/6). The threshold BER is taken to be 10^{-3} in this paper. This bit error rate is typical for the output of the Viterbi (inner) decoder in a concatenated coding scheme when the output of the (outer) Reed-Solomon decoder is about 10^{-6}. So the results given in this paper are intended to apply to the typical deep space telemetry concatenated coding scheme.

The bit rate R_b and symbol rate R_s are related by

$$R_b = \begin{cases} \frac{1}{2} R_s & \text{(7, 1/2) code} \\ \\ \frac{1}{6} R_s & \text{(15, 1/6) code.} \end{cases} \tag{1}$$

An R_b can be supported by a given P_T/N_0 if four conditions are met. The first of these is that there must be an adequate energy per bit to noise spectral density ratio at the detector. For residual-carrier telemetry, this condition is stated mathematically as

$$\frac{P_T}{N_0} \cdot \frac{\eta_{sys} \sin^2 \beta}{R_b} \geq \begin{cases} 2.98 \text{ dB} & \text{(7, 1/2) code, BER} = 10^{-3} \\ \\ 0.75 \text{ dB} & \text{(15, 1/6) code, BER} = 10^{-3}. \end{cases} \tag{2}$$

The modulation index is β, and the system loss is η_{sys}, where $0 \leq \eta_{sys} \leq 1$.[3]

The second condition is that the signal-to-noise ratio in the carrier loop must be at least 10 dB (neglecting phase noise due to transmitter frequency instability and media effects),

$$\frac{P_T}{N_0} \cdot \frac{\cos^2 \beta}{B_c} \geq 10 \text{ dB}. \tag{3}$$

B_c is the noise-equivalent bandwidth of the carrier loop.

The third condition is that the signal-to-noise ratio in the subcarrier loop must be at least 20 dB,

$$\frac{4}{\pi^2} \cdot \frac{P_T}{N_0} \cdot \frac{S_{sc} \sin^2 \beta}{W_{sc} B_{sc}} \geq 20 \text{ dB}. \tag{4}$$

This condition is necessary to minimize the loss due to imperfect subcarrier synchronization. W_{sc} ($W_{sc} \leq 1$) and B_{sc} are the subcarrier loop window factor and noise-equivalent bandwidth, respectively. B_{sc} has a maximum value of 50 Hz. S_{sc} is a squaring loss; it is given by

$$S_{sc} = \frac{2E_s/N_0}{1 + 2E_s/N_0}, \tag{5}$$

where E_s/N_0 is the energy per symbol to noise spectral density ratio,

$$\frac{E_s}{N_0} = \frac{P_T}{N_0} \cdot \frac{\sin^2 \beta}{R_s}. \tag{6}$$

The fourth condition is that the signal-to-noise ratio in the symbol loop must be at least 15 dB,

$$\frac{2}{(2\pi)^2} \cdot \frac{P_T}{N_0} \cdot \frac{S_{sym} \sin^2 \beta}{W_{sym} B_{sym}} \geq 15 \text{ dB}. \tag{7}$$

This condition is necessary to minimize the loss due to imperfect symbol synchronization. W_{sym} ($W_{sym} \leq 1$) and B_{sym} are the symbol loop window factor and noise-equivalent bandwidth, respectively. B_{sym} has a maximum value of 50 Hz. S_{sym} is a kind of squaring loss; it is a function of E_s/N_0 and W_{sym} and is given by

$$S_{sym} = \frac{\left[\text{erf}\left(\sqrt{E_s/N_0}\right) - \frac{W_{sym}}{2}\sqrt{\frac{E_s/N_0}{\pi}} \exp\left(-E_s/N_0\right)\right]^2}{1 + \frac{W_{sym}}{2}\frac{E_s}{N_0} - \frac{W_{sym}}{2}\left[\frac{1}{\sqrt{\pi}} \exp\left(-E_s/N_0\right) + \sqrt{\frac{E_s}{N_0}} \text{erf}\left(\sqrt{E_s/N_0}\right)\right]^2} \tag{8}$$

where the error function is given by

$$\text{erf}(x) = \frac{2}{\sqrt{\pi}} \int_0^x e^{-y^2}\, dy. \tag{9}$$

The squaring loss S_{sym} takes on values from 0 to 1 and asymptotically equals 1 for large values of E_s/N_0.

The largest R_b that simultaneously satisfies Inequalities (2), (3), (4), and (7) is the achievable bit rate for a given, static P_T/N_0. In practice, however, P_T/N_0 is not static but varies significantly during a tracking pass.

In all that follows, P_T/N_0 is assumed to have a profile whose shape is that of the curve shown in Figure 1. As part of the analysis leading to this paper, a family of P_T/N_0 curves were generated for X-band, with each curve having the shape shown in Figure 1 but with a different vertical displacement. The individual curves are distinguished by specifying the P_T/N_0 at zenith. The Deep Space Network also uses the Ka-band for telemetry; and the dynamic bit rate strategy of this paper also works well in that band.

The traditional telemetry playback strategy has been to use a single bit rate during the tracking pass. Figure 2 plots the best single bit rate (optimized over start/end times) as a function of zenith P_T/N_0 for the family of P_T/N_0 curves with the shape shown of Figure 1. In this figure there is one curve for each of the convolutional codes of interest here. The threshold BER is 10^{-3} and the receiver parameters are as follows: $B_c = 1$ Hz, $B_{sc} = B_{sym} = 30$ mHz, and $W_{sc} = W_{sym} = 0.25$. There is no link margin.

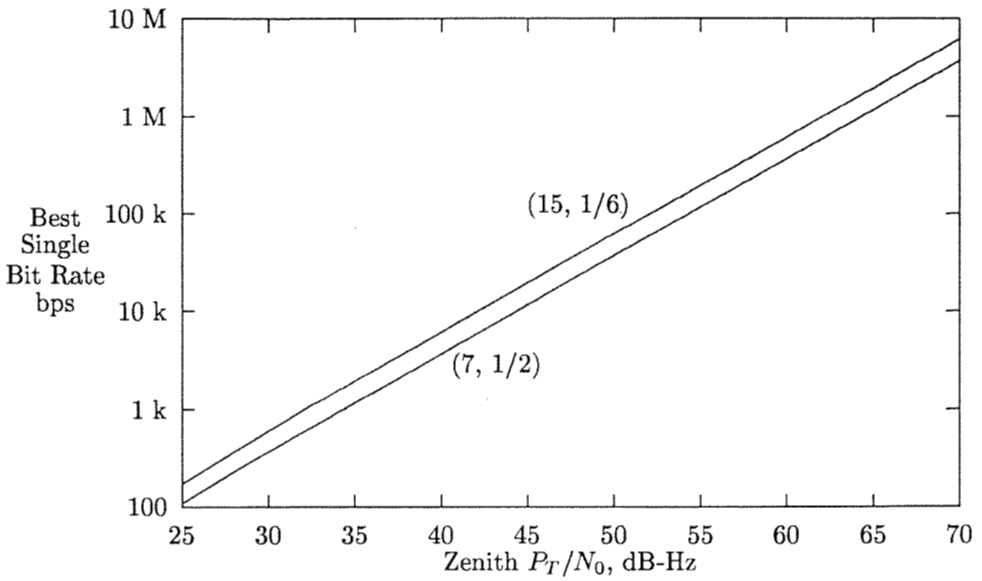

Figure 2: Best single bit rate versus zenith P_T/N_0

3 Transient Response of Subcarrier and Symbol Loops

For most of this section, a common analysis serves to characterize both the subcarrier and the symbol loop. Both loops are assumed to be third order. There is a difference, however, in how these two loops limit the symbol rate step size; this is explained toward the end of the section.

The loops are digital in implementation, and so to get the most accurate results one should really use discrete-time mathematics and take into account the update rate of the loops. However, for the sake of simplification, in this paper a continuous-time analysis is used. The results obtained in this way are quite accurate in the regime of intermediate to high bit rates.

The differential equation relating loop phase error $\phi(t)$ to input phase $\theta(t)$ is

$$\frac{d^3\phi}{dt^3} + \kappa_1 \frac{d^2\phi}{dt^2} + \kappa_2 \frac{d\phi}{dt} + \kappa_3 \phi = \frac{d^3\theta}{dt^3}, \tag{10}$$

where the coefficients are related to the noise-equivalent loop bandwidth B by [4]

$$\kappa_1 = \frac{60}{23}B, \quad \kappa_2 = \frac{4}{9}\kappa_1^2, \quad \kappa_3 = \frac{2}{27}\kappa_1^3. \tag{11}$$

A single step in phase rate, occurring at $t = 0$, is modeled as

$$\theta(t) = 2\pi \cdot \Delta f \cdot t, \quad t \geq 0, \tag{12}$$

where Δf is the phase-rate step size in cycles per second. (For the subcarrier loop, this is the change in frequency, measured in hertz. For the symbol loop, this is the symbol-rate step size, measured in symbols per second.) A solution to Eq. (10) is sought for the case of a single, isolated phase-rate step, corresponding to the $\theta(t)$ of Eq. (12). With initial conditions

$$\phi(0) = 0, \quad \frac{d\phi}{dt}(0) = 2\pi \cdot \Delta f, \quad \frac{d^2\phi}{dt^2}(0) = 0, \tag{13}$$

the solution, here denoted $\phi_1(t)$, is

$$\phi_1(t) = \frac{2\pi \cdot \Delta f}{p} \left[2 - 2\cos(pt) + \sin(pt)\right] e^{-pt}, \quad t \geq 0, \tag{14}$$

where

$$p = \frac{\kappa_1}{3} = \frac{20}{23} B. \tag{15}$$

Figure 3 shows an example of the phase error transient response to a single step in phase rate occurring at $t = 0$ with Δf chosen so that the peak phase error is 0.1 radian.

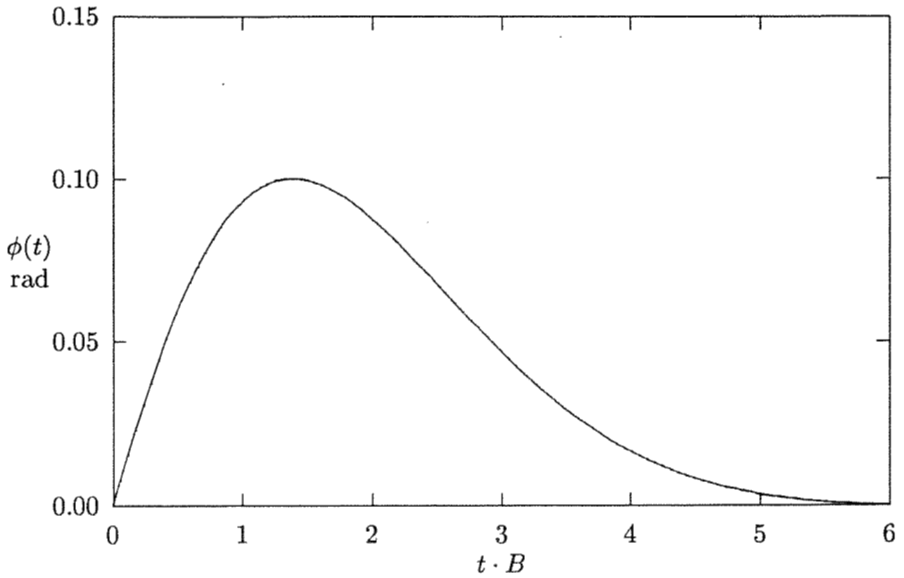

Figure 3: $\phi_1(t)$ versus $t \cdot B$

A solution of Eq. (10) is also sought for the case of periodic steps in phase rate. The steps are here assumed to be all of the same size and spaced T seconds apart. The solution, in this case, is periodic with period T. For the interval $0 \le t \le T$, the solution is

$$\sum_{n=0}^{\infty} \phi_1(t + nT), \qquad 0 \le t \le T.$$

It is of interest to know the peak value ϕ_{peak} of phase error; this is given by

$$\phi_{peak} = \frac{2\pi \cdot \Delta f}{p} \Lambda(pT), \tag{16}$$

where

$$\Lambda(pT) = \max_{pt} \sum_{n=0}^{\infty} [2 - 2\cos(pt + pnT) + \sin(pt + pnT)]\, e^{-(pt+pnT)}. \tag{17}$$

$\Lambda(pT)$ may be characterized for large values of pT as follows. For $pT \gg 1$, only the $n = 0$ term makes a significant contribution to the sum, and $\Lambda(pT)$ becomes approximately

$$\begin{aligned} \Lambda(pT) &\approx \max_{pt} [2 - 2\cos(pt) + \sin(pt)]\, e^{-pt} \\ &\approx 0.665, \qquad pT \gg 1. \end{aligned} \tag{18}$$

$\Lambda(pT)$ may also be characterized for small values of pT. For $pT \ll 1$, the sum becomes independent of t; it is necessary only to consider one example value of t. In order to simplify the mathematics, $t = 0$ is chosen.

$$\Lambda(pT) \approx \frac{1}{pT} \lim_{pT \to 0} \sum_{n=0}^{\infty} [2 - 2\cos(pnT) + \sin(pnT)]\, e^{-pnT}\, pT$$

$$\approx \frac{1}{pT}\int_0^\infty (2-2\cos x+\sin x)\,e^{-x}\,dx$$
$$\approx \frac{3}{2pT}, \quad pT \ll 1. \tag{19}$$

In general, neither the approximation of Eq. (18) nor that of Eq. (19) is valid, then $\Lambda(pT)$ must be evaluated numerically from Eq. (17).

It is assumed here that the subcarrier frequency and the symbol rate are coherently generated from the same frequency source and that the former is exactly 5 times the latter. The new transponder currently being developed for future deep space missions has been designed to provide such capabilities. The ratio of 5 is expected to be typical for future deep space missions. In this analysis, the maximum permissible step change in symbol rate is taken to be that which satisfies

$$\Delta R_s = \min\left(\frac{0.1\,p_{sym}}{2\pi\Lambda(p_{sym}T)}, \frac{0.1\,p_{sc}}{5\cdot 2\pi\Lambda(p_{sc}T)}\right). \tag{20}$$

The parameters p_{sc} and p_{sym} are given by

$$p_{sym} = \frac{20}{23}B_{sym} \tag{21}$$
$$p_{sc} = \frac{20}{23}B_{sc}, \tag{22}$$

where B_{sym} and B_{sc} are the noise-equivalent bandwidths of the symbol and subcarrier loops, respectively. In words, the periodic step changes in symbol rate shall not cause the peak phase error in either the symbol loop or the subcarrier loop to exceed 0.1 rad. The subcarrier loop is an issue here because changing the symbol rate also changes the subcarrier frequency, since the two are coherently related. The assumption of a 5:1 ratio between subcarrier frequency and symbol rate manifests itself in Eq. (20) as the factor of 5 in the denominator of the second term within the minimum function.

4 Changing the Bit Rate During a Tracking Pass

Based on the analysis of the two previous sections, a strategy is proposed for increasing total data return of a tracking pass above that which is possible by using the best single bit rate. The proposed strategy features a dynamic bit rate. R_b is increased by periodic, small steps. Actually, there are two versions of this strategy. In the first version, R_b is stepped once each telemetry frame. In a second version, R_b is increased once each symbol. With either version of this strategy, no predicts of the bit rate steps are required by the receiver because the symbol loop can track out these steps with acceptable transient phase error. It has been experimentally verified that the Deep Space Network's workhorse receiver, the Block-V Receiver, can track small bit rate changes without loss of synchronization. [2]

The step size of R_b is limited by the following constraints:

1. R_b must not exceed the maximum bit rate achievable for a given P_T/N_0. In other words, R_b must, at every point in time, satisfy Inequalities (2), (3), (4), and (7).

2. The corresponding symbol step size must have an absolute value less than or equal to the ΔR_s given by Eq. (20). In that equation, T is the time between two successive steps.

ϕ_{peak} is chosen, rather conservatively, to be 0.1 radian. For such a ϕ_{peak} the effective signal-to-noise ratio loss is negligible and the subcarrier and symbol loops are unlikely to slip cycles. Certainly, larger values of ϕ_{peak} could be tolerated, but then the signal-to-noise ratio loss would be significant and occasional cycle slips would occur; it would then be necessary to estimate these impairments.

The bandwidths B_{sc} and B_{sym} are constants for each tracking pass. B_{sc} is chosen as the largest value satisfying Inequality (4) at the start time for the tracking pass, subject to the existing hardware constraint

$$B_{sc} \leq 50 \text{ Hz}. \tag{23}$$

B_{sym} is chosen as the largest value satisfying Inequality (7) at the start time for the tracking pass, subject to the existing hardware constraint

$$B_{sym} \leq 50 \text{ Hz}. \tag{24}$$

These upper limits on B_{sc} and B_{sym} are valid for the Block-V Receiver. It is important to use the largest permissible B_{sc} consistent with Inequality (23) and a subcarrier loop signal-to-noise ratio of 20 dB and to use the largest permissible B_{sym} consistent with Inequality (24) and a symbol loop signal-to-noise ratio of 15 dB; this maximizes the bit rate step size allowed by constraint 2.

The modulation index is taken to be constant during a tracking pass. In principle, the optimum modulation index is a function of the bit rate, so there is some gain to be had by adjusting the modulation index along with the bit rate; but in practice this gain is very small. The modulation index is chosen to be optimum at zenith.

Figure 4 shows R_b as a function of time during a tracking pass for the above dynamic R_b strategy in the case of a P_T/N_0 profile of the shape given in Figure 1 and a zenith P_T/N_0 of 53 dB-Hz. For this figure, a (7, 1/2) code is used and the threshold BER is 10^{-3}. There is no link margin. The curve labeled "maximum" in that figure is the achievable static bit rate for the instantaneous value of P_T/N_0; this is an upper bound to what may be achieved by a practical dynamic R_b strategy. The curve labeled "best single rate" illustrates the traditional strategy of using just one bit rate that has been optimized over start/end times. (This optimization amounts to a simple geometric proposition: of all the rectangles that fit completely under the "maximum" curve, the one with the largest area has a height equal to the best single bit rate and an area equal to the total data return.) The curve labeled "symbol" shows what can be achieved by using the dynamic R_b strategy with a bit rate step every symbol. The receiver parameters assumed in the generation of this curve are as follows: $B_c = 1$ Hz and $W_{sc} = W_{sym} = 0.25$. An optimization was done over start/end times, and the bandwidths B_{sc} and B_{sym} were chosen as described above. In optimizing the start/end times, there are two advantages of starting later and ending earlier: the starting R_b is larger; and B_{sc} and B_{sym} are larger, permitting larger bit rate steps. There is, of course, one obvious advantage to starting earlier and ending later: there is more time to collect bits.

The ratio, in decibels, of the total bits returned by the dynamic R_b strategy to the total bits returned by the best single rate strategy (for a common P_T/N_0 profile) is used in this paper as a figure-of-merit for the dynamic R_b strategy. For example, the "symbol" curve of Figure 4 yields 0.92 dB more total bits for the tracking pass than does the best single rate strategy.

Figure 5 shows the gain, as defined in the previous paragraph, for the dynamic R_b strategy relative to the best single rate strategy for the case of a (7, 1/2) code and a threshold BER of 10^{-3}. This one figure shows the gain for an entire family of P_T/N_0 profiles. The abscissa is the zenith P_T/N_0, and the ordinate is the gain relative to the best single rate strategy. The curve labeled "maximum" is not achievable in practice; it represents the hypothetical case where only constraint 1 is a consideration, not constraint 2. (This is what the gain would be if the P_T/N_0 profile could be matched exactly.) The curve labeled "frame" is for the dynamic R_b strategy with bit rate changes once per frame with a frame size of 10232 bits. The curve labeled "symbol" is for the dynamic R_b strategy with bit rate changes once per symbol. For Figure 5, the receiver parameters are as follows: $B_c = 1$ Hz and $W_{sc} = W_{sym} = 0.25$. As before, there is no link margin.

Beginning with 25 dB-Hz, the gain of the dynamic R_b strategy increases as the zenith P_T/N_0 increases: the dynamic R_b strategy does an increasingly better job of hugging the maximum R_b curve (that is based only on constraint 1). The once-per-symbol approach gives larger gains than does the once-per-frame approach. Both curves level off and finally begin to fall. For small and intermediate values of zenith P_T/N_0 (corresponding to small and intermediate values for best single bit rate), the dynamic R_b strategy with changes bit rate changes each symbol works quite well. On

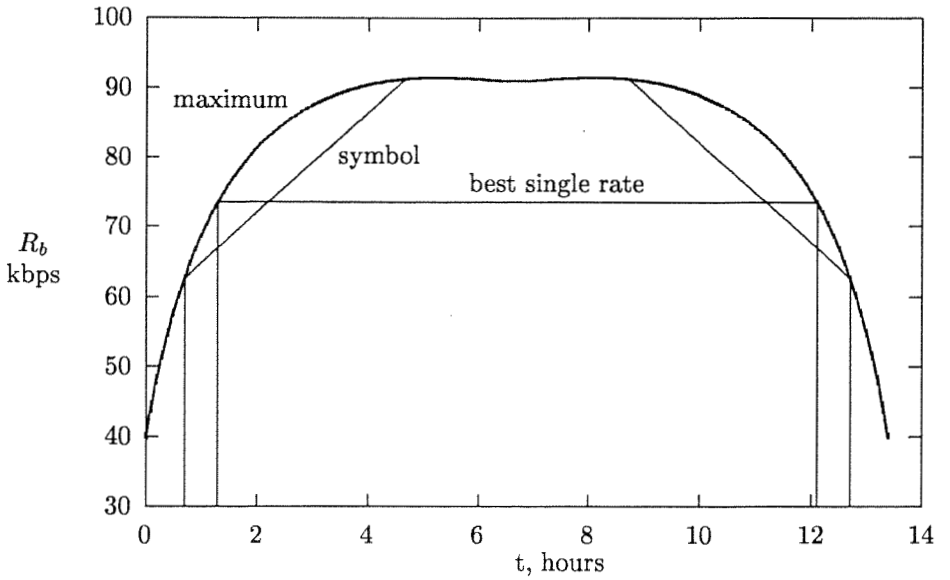

Figure 4: R_b variation during a tracking pass; zenith $P_T/N_0 = 53$ dB-Hz, (7, 1/2) code

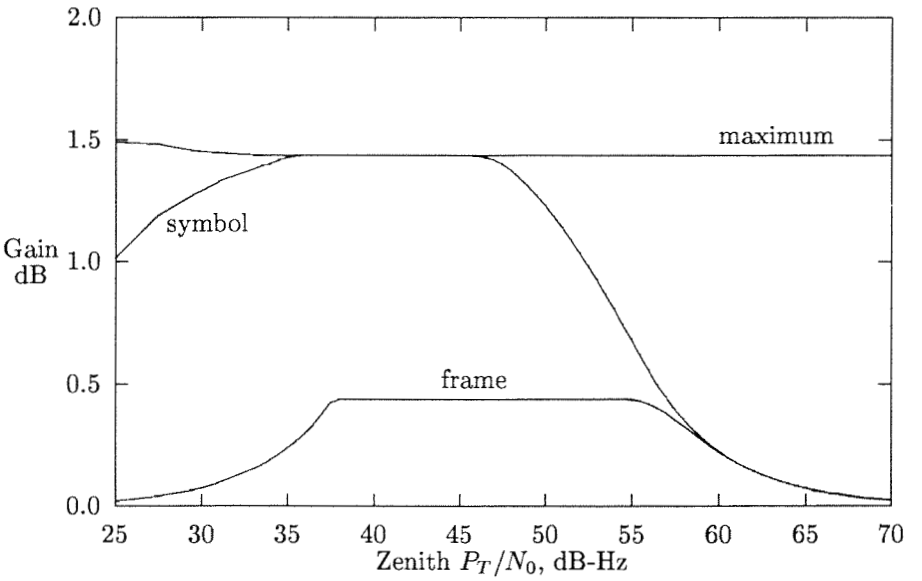

Figure 5: Gains relative to single-rate strategy; (7, 1/2) code

the other hand, for large values of zenith P_T/N_0 (corresponding to large values for best single bit rate), the dynamic R_b strategy offers little advantage over the traditional strategy of using the best single bit rate. If in this analysis a less conservative value had been used for ϕ_{peak} (i.e., if a larger ϕ_{peak} had been used), then the same qualitative conclusions would apply; but there would be a wider range of values for zenith P_T/N_0 that give high gain.

For small values of zenith P_T/N_0, the dynamic R_b strategy does not offer much gain because B_{sc} and B_{sym} must be very small in order to achieve acceptable subcarrier and symbol loop signal-to-noise ratios, but as a result only small steps in R_b can be tolerated. For intermediate values of zenith P_T/N_0, B_{sc} and B_{sym} are large enough to permit significant step sizes in R_b. For large values of zenith P_T/N_0, B_{sc} and B_{sym} are constrained by Ineqs. (23) and (24) and the dynamic R_b strategy does not offer much gain; this is not a serious concern because for large R_b there are better signal structures to use than the one considered in this paper. (In particular, the subcarrier is unnecessary for large R_b.)

The gain of a dynamic R_b strategy could be better if the subcarrier frequency and symbol rate were not harmonically related, so that the symbol rate could be dynamic while the subcarrier frequency is static. However, there are unrelated practical reasons for preferring the harmonic relationship.

Figure 6 shows gain with the dynamic R_b strategy as a function of zenith P_T/N_0 when a (15, 1/6) code is used. Comparison of Figure 6 with Figure 5 makes it clear that, in general, more is to be gained with a dynamic R_b strategy when using the rate 1/2 code than when using the rate 1/6 code. The reason for this is that for a given bit rate the symbol rate is higher with the rate 1/6 code than it is for the rate 1/2 code. Therefore, E_s/N_0 is lower and the squaring losses in the subcarrier and symbol loops are worse for the rate 1/6 code. As compensation, B_{sc} and B_{sym} must be smaller for the rate 1/6 code; and, therefore, the ability to track dynamic R_b is compromised.

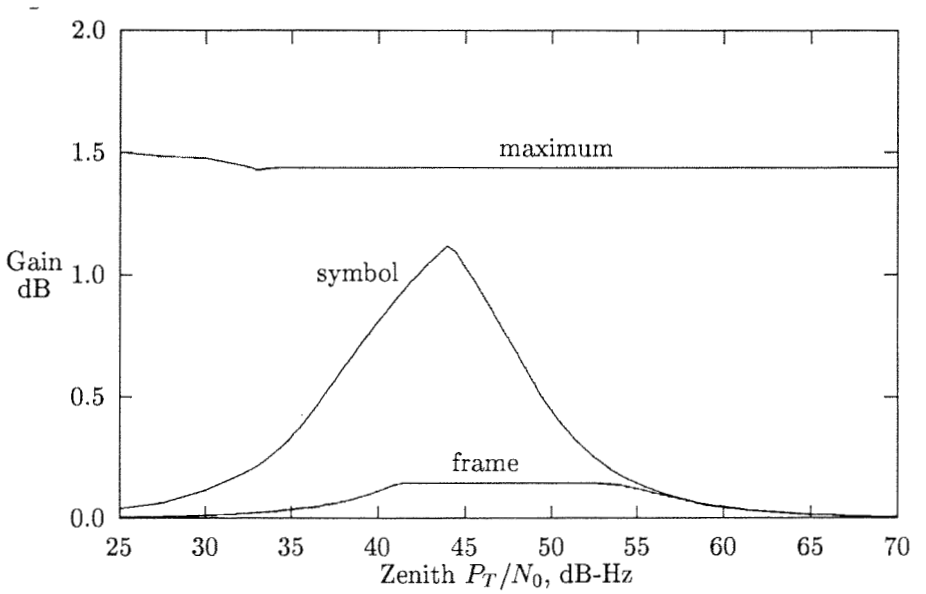

Figure 6: Gains relative to single-rate strategy; (15, 1/6) code

5 Conclusions

Changing the bit rate during a tracking pass can result in significant increases in total data return relative to a single rate strategy (especially when the changes are once-per-symbol). The bit rate can be changed in small steps so that the receiver subcarrier and symbol loops have only small

transient phase errors. No very precise predictions of the subcarrier frequency and symbol rate changes need be made available to the receiver. This dynamic R_b strategy works well for those tracking passes for which the best single rate is of intermediate value. For example, for once-per-symbol changes with the (7, 1/2) code, the dynamic R_b strategy yields significant gain for tracking passes having best single bit rates between about 100 bps and 100 kbps.

6 Acknowledgment

The research described in this paper was carried out at the Jet Propulsion Laboratory, California Institute of Technology, under a contract with the National Aeronautics and Space Administration.

References

[1] S. D. Slobin and M. K. Sue, "DSN 34-m Beam-Waveguide Antenna Gain and Noise Temperature Models for Telecom Systems Analysis," Report D–11591, Jet Propulsion Laboratory, Pasadena, California, March 1, 1994.

[2] M. K. Sue, *et al.*, "Increased Suppressed-Carrier Telemetry Return by Means of Frequent Changes in Bit Rate During a Tracking Pass," *The Telecommunications and Mission Operations Progress Report 42–137*, Jet Propulsion Laboratory, Pasadena, California, May 15, 1999. *http://tmo.jpl.nasa.gov/progress_report*

[3] "TLM-21: DSN Telemetry System, Block-V Receiver," December 1, 1996, in Document 810-5, *Deep Space Network / Flight Project Interface Design Handbook*, Vol. I, Jet Propulsion Laboratory, Pasadena, California. *http://deepspace1.jpl.nasa.gov/810-5*

[4] S. A. Stephens and J. B. Thomas, "Controlled-Root Formulation for Digital Phase-Locked Loops," *IEEE Transactions on Aerospace and Electronic Systems*, Vol. 31, No. 1, pp. 78–95, January 1995.